

Shape sensitivity analysis for the optimal perforation problem in acoustic transmission

Eduard Rohan^a, Vladimír Lukeš^b

^{a,b} Department of Mechanics, Faculty of Applied Sciences, University of West Bohemia,
Univerzitní 22, 30614 Plzeň, Czech Republic
E-mail: ^arohan@kme.zcu.cz
^blukes@kme.zcu.cz

1. Abstract

We consider the acoustic transmission through perforated interface separating two halfspaces occupied by the acoustic medium. Recently the homogenized transmission conditions were obtained as the two-scale homogenization limit of the standard acoustic problem imposed in the layer perforated by a sieve-like obstacle with periodic structure. The limit model involves homogenized impedance coefficients depending on the so-called microscopic problems; these are imposed in the reference computational cell, Y embedding obstacle S the shape of which can be designed. We focus on the sensitivity of the homogenized coefficients w.r.t. shape modification of the perforation represented by S ; sensitivity formulas are reported and illustrated by numerical examples. This research will contribute to the complex tasks, such as minimization of the transmission loss computed in a domain embedding this perforated interface.

2. Keywords: linear acoustics, homogenization, transmission condition, sensitivity analysis

3. Introduction

Minimization of noise produced by flowing acoustic medium (inviscid compressible fluid) belongs to important challenges of the aerospace and automotive engineering. For example, in the exhaust silencers of the combustion engines the gas flows through ducts equipped with various sieve-like structures which in part may influence the transmission losses associated with acoustic waves propagating in the exhaust gas. Apart from optimization of the exhaust silencers, obviously there are other devices involving sieve-like structures for which the acoustic transmission is an important figure to look at.

We have in mind an optimal design problem aimed at minimization of a cost functional which depends on the overall acoustic pressure field; this field is the solution of the acoustic problem imposed in a domain subdivided into two parts by the perforated thin (but rigid) structure, which is represented by the corresponding mid-surface Γ_0 . The transmission condition on the mid-surface is presented in an implicit form by the system of the surface-wave equation constrained by pressure jump of the two pressure field traces. The transmission condition involves two interface variables: the surface acoustic pressure and the transversal acoustic momentum; the latter couples the acoustic pressure fields in both the domains in the form of the Neumann condition.

The transmission condition (imposed on the interface planar mid-surface) was recently derived using the asymptotic analysis. In the homogenized form, the perforated thin structure, having possibly quite complex form of the perforation, is represented by some homogenized impedance coefficients depending on the so-called microscopic problems; they are solved in the reference computational cell Y embedding obstacle S the shape of which can be designed.

Acoustic response to the global acoustic problem involving the transmission conditions is subject to the sensitivity analysis. Namely the total variation of the transmission loss w.r.t. shape of S at the “microlevel” is derived. By virtue of the state problem hierarchical structure the complex sensitivity can be developed at three levels: 1) shape sensitivity of the homogenized coefficient at the microscopic level; 2) “material” sensitivity (w.r.t. perturbation of the homogenized coefficients) of the interface variables associated with interface wave equation; 3) sensitivity associated with control problem: to optimize the overall pressure field distribution using the interface variables variation. The sensitivity of the “upper level” problem, i.e. 2) and 3), requires solving an adjoint equation; this issue has been addressed in [5]. Here we deal with the sensitivity for the “lower level” problem which associates the microstructure geometry, i.e. the perforation design, with the effective (homogenized) transmission coefficients of the upper level problem.

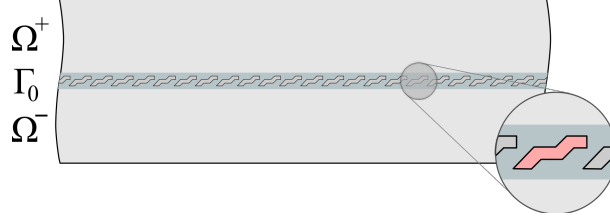


Figure 1: Acoustic domain Ω divided by perforated plane Γ_0 .

We consider the acoustic medium occupying domain Ω which is subdivided by perforated plane Γ_0 in two disjoint subdomains Ω^+ and Ω^- , so that $\Omega = \Omega^+ \cup \Omega^- \cup \Gamma_0$, see Fig. 1. In a case of no convection flow (the linear acoustics), the acoustic waves in Ω are described by the following equations

$$\begin{aligned}
 & c^2 \nabla^2 p + \omega^2 p = 0 \quad \text{in } \Omega^+ \cup \Omega^-, \\
 \text{transmission conditions} & \quad \begin{cases} c^2 \frac{\partial p}{\partial n^+} = i\omega g_0 \\ c^2 \frac{\partial p}{\partial n^-} = -i\omega g_0 \end{cases} \quad \text{on } \Gamma_0, \\
 \text{boundary conditions} & \quad \text{on } \partial\Omega.
 \end{aligned} \tag{1}$$

where $\frac{\partial p}{\partial n^\pm} = n^\pm \cdot \nabla p$ are the normal derivatives on Γ_0 w.r.t. normals outward to Ω^+ and Ω^- , respectively. The transmission conditions on interface Γ_0 involve the transversal acoustic momentum g_0 ; this variable satisfies additional integral identities that were developed in [7] using the asymptotic analysis.

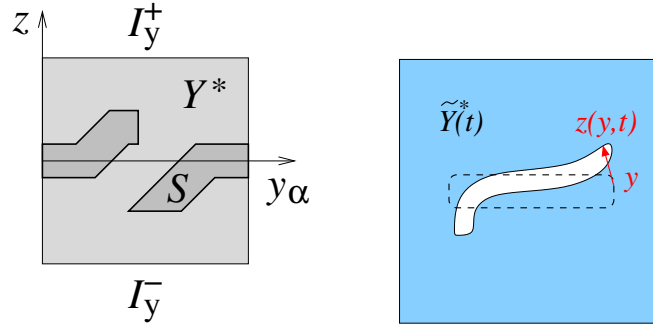


Figure 2: Left: design velocity field is supported in Y^* , boundary ∂S is shaped by design parameters. Right: Domain perturbation using (10); parameter t corresponds to τ used in the text.

4. Optimal perforation design problem

In this section we shall formulate problem of optimal shape of the periodic perforations targeted to maximize the transmission loss measured in an acoustic device which is equipped with the perforated interface. The state problem has a hierarchical structure incorporating *two levels*. In this paper we focus on the lower level which associates the perforation geometry with the *homogenized coefficients* of the transmission conditions. They are introduced below using so called corrector functions defined in the reference periodic cell $Y =]0, 1[\times] -1/2, +1/2[$, $Y \subset \mathbb{R}^3$. The acoustic medium occupies domain $Y^* = Y \setminus S$, where $S \subset Y$ is the solid (rigid) obstacle, see Fig. 2. For clarity we use notation $I_y =]0, 1[$. The upper and lower boundaries are translations of $(I_y, 0)$; we define $I_y^+ = \{y \in \partial Y : z = 1/2\}$ and $I_y^- = \{y \in \partial Y : z = -1/2\}$. By $H_{\#(1,2)}^1(Y)$ we denote the space of $H^1(Y)$ functions which are “1-periodic” in coordinates y_α , $\alpha = 1, 2$; such functions will be called “transversely Y-periodic”.

4.1 Upper level state problem

Let p be the acoustic pressure in $\Omega = \Omega^+ \cup \Omega^- \cup \Gamma_0$ and p^+ , p^- be traces of $p|_+$, $p|_-$ on Γ_0 , respectively, where $p|_\pm$ are restrictions of p on Ω^\pm . Thus, the acoustic pressure is discontinuous across Γ_0 ; we shall

need the space

$$H^1(\Omega \setminus \Gamma_0) = L^2(\Omega) \cap (H^1(\Omega^+) \cup H^1(\Omega^-)) .$$

The *upper level state problem* is to find $p \in H^1(\Omega \setminus \Gamma_0)$ and the interface related functions $p^0 \in H^1(\Gamma_0)$ and $g^0 \in L^2(\Gamma_0)$ such that for a given $\bar{p} \in L^2(\Gamma_{\text{in}})$ the following holds:

$$a_\Omega(p, q) - \omega^2(p, q)_\Omega + \omega c \langle p, q \rangle_{\Gamma_{\text{in-out}}} - i\omega \langle g^0, q^+ \rangle_{\Gamma_0} + i\omega \langle g^0, q^- \rangle_{\Gamma_0} = 2i\omega c \langle \bar{p}, q \rangle_{\Gamma_{\text{in}}} \quad (2)$$

for all $q \in H^1(\Omega \setminus \Gamma_0)$, and

$$\begin{aligned} \mathcal{A}(p^0, \phi) - \omega^2 \varsigma^* \langle p^0, \phi \rangle_{\Gamma_0} + i\omega \mathcal{B}(g^0, \phi) &= 0, \quad \forall \phi \in H^1(\Gamma_0), \\ -i\omega \varkappa_0 \mathcal{B}(\psi, p^0) + \omega^2 \mathcal{F}(g^0, \psi) &= -i\omega \frac{1}{\varepsilon_0} \langle p^+ - p^-, \psi \rangle_{\Gamma_0}, \quad \forall \psi \in L^2(\Gamma_0), \end{aligned} \quad (3)$$

where $\varsigma^* = |Y^*|/|Y|$ is related to porosity of the perforation, $\varkappa_0 = \varkappa/|I_y|$ is the dilatation parameter (≈ 1 , see [7]), the bilinear forms involved in (2) are, as follows

$$\begin{aligned} a_\Omega(p, q) &= \int_\Omega c^2 \nabla p \cdot \nabla q, \\ (p, q)_\Omega &= \int_\Omega pq, \\ \langle p, q \rangle_\Gamma &= \int_\Gamma pq \, d\Gamma, \end{aligned} \quad (4)$$

and the bilinear forms involved in (3) are defined in terms of the homogenized coefficients $A_{\alpha\beta}$, B_α and F , ($\alpha = 1, 2$ for 3D problems) which will be defined in the next paragraph:

$$\begin{aligned} \mathcal{A}(p, q) &= \int_{\Gamma_0} A_{\alpha\beta} \partial_\beta p \partial_\alpha q \, d\Gamma, \\ \mathcal{B}(g, q) &= \int_{\Gamma_0} B_\alpha g \partial_\alpha q \, d\Gamma, \\ \mathcal{F}(g, h) &= \int_{\Gamma_0} Fgh \, d\Gamma. \end{aligned} \quad (5)$$

4.2 Microscopic problems

The homogenized coefficients, A, B, F and, thereby, the bilinear forms $\mathcal{A}, \mathcal{B}, \mathcal{F}$ are determined by the solution of the *level 3 state problem* constituted by the local corrector problems. To simplify the notation, we introduce

$$\begin{aligned} \hat{\nabla} q &= (\partial_\alpha^y q, \varkappa^{-1} \partial_z q), \\ a_Y^*(\pi, \xi) &= \int_{Y^*} \hat{\nabla} \pi \cdot \hat{\nabla} \xi = \int_{Y^*} \left(\partial_\alpha^y \pi \partial_\alpha^y \xi + \frac{1}{\varkappa^2} \partial_z \pi \partial_z \xi \right), \\ \gamma^\pm(\xi) &= \int_{I_y^+} \xi - \int_{I_y^-} \xi \end{aligned} \quad (6)$$

and rewrite the local corrector problems as follows: Find $\pi^\beta, \xi \in H_{\#(1,2)}^1(Y)/\mathbb{R}$ such that

$$\begin{aligned} a_Y^*(\pi^\beta + y_\beta, \phi) &= 0, \quad \forall \phi \in H_{\#(1,2)}^1(Y), \quad \beta = 1, 2, \\ a_Y^*(\xi, \phi) &= -\frac{|Y|}{\varkappa c^2} \gamma^\pm(\phi), \quad \forall \phi \in H_{\#(1,2)}^1(Y). \end{aligned} \quad (7)$$

Using the notation just introduced, the homogenized coefficients can be expressed, as follows:

$$\begin{aligned} A_{\alpha\beta} &= \frac{c^2}{|Y|} a_Y^*(\pi^\beta + y^\beta, \pi^\alpha + y^\alpha), \\ B_\alpha &= \frac{c^2}{|Y|} a_Y^*(\xi, y_\alpha), \\ F &= \frac{1}{|I_y|} \gamma^\pm(\xi). \end{aligned} \quad (8)$$

We can now define the *optimal perforation design problem*:

$$\begin{aligned} & \min_{\alpha \in D_{adm}} \Phi(p) \\ \text{subject to: } & p \text{ solves (2)-(3),} \\ & \text{where } A, B, F \text{ are given by (7)-(8).} \end{aligned} \tag{9}$$

D_{adm} is the set of admissible designs; besides shape smoothness requirements it should reflect some constraints concerning the size of the obstacle (thickness) and porosity of the interface.

5. Shape sensitivity analysis at the lower level

We shall present general sensitivity formulas for the homogenized coefficients A, B, F .

5.1 Elements of material and shape derivatives

We are interested in variation of the shape of the obstacle S placed in the domain, Y , thereby in variation of $Y^* \subset Y$. On introducing the velocity field $\vec{\mathcal{V}}$ in Y we parameterize the material points constituting the domain Y by

$$z_i(y, \tau) = y_i + \tau \mathcal{V}_i(y), \quad y \in Y, \quad i = 1, 2, \tag{10}$$

where τ is the “time-like” variable, see Fig. 2; for all details on the concept of shape and material derivatives we refer to [4] and [3]. Throughout the text below we shall use the notion of the following derivatives:

$$\begin{aligned} \delta(\cdot) & \dots \text{ total (material) derivative} \\ \delta_\tau(\cdot) & \dots \text{ partial (local) derivative w.r.t. } \tau. \end{aligned}$$

The derivatives just introduced are computed as the directional derivatives in the direction of $\vec{\mathcal{V}}(y)$, $y \in Y$; for reader’s convenience we recall the definitions of both the material and local derivatives, as considered e.g. in [3]. Let $f(y)$ be a smooth function, e.g. $f \in C^1(Z)$, where $Z \supset Y$ is such that for τ small enough $z_i(y, \tau) \in Z$ for any $y \in Y$. We assume that f depends on the actual shape of Y which is perturbed by the velocity field $\vec{\mathcal{V}}$, as introduced in (10). Therefore, by $\tilde{f}(z, \tau)$ we denote the function value evaluated at $z = z(\tau)$ and associated with the perturbed design $Y(\tau) = \{z \mid z(y, \tau) = y + \tau \mathcal{V}(y), y \in Y\}$. Due to mapping (10) one can trace the ”motion” of a selected material point. The *material derivative* reflects the change of the function value in the material point which is convected with velocity \mathcal{V} :

$$\begin{aligned} \delta f(y) \circ \mathcal{V} & \equiv \lim_{\tau \rightarrow 0_+} \frac{\tilde{f}(z(y, \tau), \tau) - f(y)}{\tau} \\ & = \lim_{\tau \rightarrow 0_+} \frac{\tilde{f}(z(y, \tau), \tau) - \tilde{f}(y, \tau)}{\tau} + \lim_{\tau \rightarrow 0_+} \frac{\tilde{f}(y, \tau) - f(y)}{\tau} \\ & = \delta_\tau f(y) \circ \mathcal{V} + \nabla f(y) \cdot \mathcal{V}(y), \end{aligned} \tag{11}$$

where the *partial derivative* is defined by

$$\delta_\tau f(y) \circ \mathcal{V} = \lim_{\tau \rightarrow 0_+} \frac{\tilde{f}(y, \tau) - f(y)}{\tau}, \tag{12}$$

so that it corresponds to the local change in f evaluated at fixed position $y \in Y$.

Once the shap variation $\delta \partial S$ is defined, velocities \mathcal{V} can be established in Y^* by various methods; very often an auxiliary elasticity problem is solved in Y^* .

5.2 Shape sensitivity of the homogenized transmission coefficients

Through the following text, for simplicity of the notation, we shall write just $\delta_\tau(\cdot)$ and $\delta(\cdot)$ instead of $\delta_\tau(\cdot) \circ \mathcal{V}$ and $\delta(\cdot) \circ \mathcal{V}$, respectively, to refer to the directional derivatives (11)-(12).

We shall derive sensitivity formulae for computing the shape derivatives of the homogenized coefficients defined in (8). For this we need to differentiate the local equations (7); thus, we obtain

$$\begin{aligned} \delta_\tau a_Y^*(\pi^\alpha, \phi) \circ \mathcal{V} + a_Y^*(\delta \pi^\alpha \circ \mathcal{V} + \mathcal{V}_\alpha, \phi) & = 0, \\ \delta_\tau a_Y^*(\xi, \phi) \circ \mathcal{V} + a_Y^*(\delta \xi \circ \mathcal{V}, \phi) & = 0, \end{aligned} \tag{13}$$

for all $\phi \in H_{\#(1,2)}^1(Y)$, where

$$\begin{aligned}\delta_\tau a_Y^*(\phi, \psi) \circ \mathcal{V} &= \int_{Y^*} \left[\operatorname{div} \mathcal{V} \hat{\nabla} \phi \cdot \hat{\nabla} \psi - (\hat{\nabla} \mathcal{V} \cdot \nabla \phi) \cdot \hat{\nabla} \psi - \hat{\nabla} \phi \cdot (\hat{\nabla} \mathcal{V} \cdot \nabla \psi) \right] \\ &= \int_{Y^*} \left[\operatorname{div} \mathcal{V} \hat{\nabla} \phi \cdot \hat{\nabla} \psi - \partial_\alpha \mathcal{V}_k \partial_k \phi \partial_\alpha \psi - \partial_\alpha \phi \partial_\alpha \mathcal{V}_l \partial_l \psi \right. \\ &\quad \left. - \frac{1}{\varkappa^2} \partial_z \mathcal{V}_k \partial_k \phi \partial_z \psi - \frac{1}{\varkappa^2} \partial_z \phi \partial_z \mathcal{V}_l \partial_l \psi \right].\end{aligned}\quad (14)$$

This expression is derived by virtue of the definition in (11),

$$\begin{aligned}\delta_\tau a_Y^*(\pi, \phi) &= \lim_{\tau \rightarrow 0} \tau^{-1} \left[a_{Y(\tau)}^*(\pi, \phi) - a_Y^*(\pi, \phi) \right] \\ \text{where } a_{Y(\tau)}^*(\pi, \phi) &= \int_{Y^*} \left[\frac{\partial y_k}{\partial z_\alpha} \frac{\partial \pi}{\partial y_k} \frac{\partial y_l}{\partial z_\alpha} \frac{\partial \phi}{\partial y_l} + \frac{1}{\varkappa^2} \frac{\partial y_k}{\partial z_3} \frac{\partial \pi}{\partial y_k} \frac{\partial y_l}{\partial z_3} \frac{\partial \phi}{\partial y_l} \right] J(z).\end{aligned}$$

On differentiating (8) we obtain the sensitivity of $A_{\alpha\beta}$:

$$\delta A_{\alpha\beta} \circ \mathcal{V} = \frac{c^2}{|Y|} \left[\delta_\tau a_Y^*(\pi^\beta + y_\beta, \pi^\alpha + y_\alpha) \circ \mathcal{V} + a_Y^*(\mathcal{V}_\beta, \pi^\alpha + y_\alpha) + a_Y^*(\pi^\beta + y_\beta, \mathcal{V}_\alpha) \right] \quad (15)$$

where the following identity was employed $a_Y^*(\pi^\beta + y_\beta, \delta\pi^\alpha) = 0$. From this and using (13)₂ one obtains

$$a_Y^*(\delta\xi, y_\beta) = -a_Y^*(\delta\xi, \pi^\beta) = \delta_\tau a_Y^*(\xi, \pi^\beta), \quad (16)$$

which is used to simplify the sensitivity of B_α :

$$\begin{aligned}\delta B_\alpha \circ \mathcal{V} &= \frac{c^2}{|Y|} \left[a_Y^*(\delta\xi \circ \mathcal{V}, y_\alpha) + a_Y^*(\xi, \mathcal{V}_\alpha) + \delta_\tau a_Y^*(\xi, y_\alpha) \circ \mathcal{V} \right] \\ &= \frac{c^2}{|Y|} \left[\delta_\tau a_Y^*(\xi, \pi^\alpha + y_\alpha) \circ \mathcal{V} + a_Y^*(\xi, \mathcal{V}_\alpha) \right].\end{aligned}\quad (17)$$

In order to derive the sensitivity of F , we apply subsequently (7)₂ with $\phi = \delta\xi$ and (13)₂, thus

$$\delta F \circ \mathcal{V} = \frac{1}{|I_y|} \gamma^\pm(\delta\xi) \circ \mathcal{V} = -\frac{\varkappa c^2}{|I_y||Y|} a_Y^*(\xi, \delta\xi) \circ \mathcal{V} = \frac{\varkappa c^2}{|I_y||Y|} \delta_\tau a_Y^*(\xi, \xi) \circ \mathcal{V}. \quad (18)$$

6. Numerical examples

This section presents some illustrative numerical examples of acoustic transmission showing influence of the perforation design. Examples were computed using our code based on Python language (“Sfepy” project, [2]).

6.1 Various perforations in 3D

In Fig. 3, we compare the corrector functions ξ^\pm , π and homogenized parameters A , B , F of three different perforations in 3D. Due to the geometrical arrangement of the solid obstacles the coupling coefficients B , D vanish for perforation types 3D/#1 and 3D/#2. For type 3D/#3 these coefficients are nonzero, i.e. the transversal and tangential velocities in the interface layer are coupled.

6.2 Sensitivity of the homogenized coefficients

The shape sensitivity of the homogenized transmission coefficients was tested in 2D with the simple geometry of the periodic perforation. In Fig. 4 we tested the sensitivity with respect to rotation of the solid rectangular obstacle. The sensitivity coefficients δA , δB and δF are shown for unrotated and rotated solid obstacle.

7. Conclusion

The “multi-scale” homogenization approach was employed and envisaged for an efficient treatment of the optimal perforation design. The model and its sensitivity discussed in this paper are implemented in our in-house developed finite element based code SfePy ([2]). In [7], using the asymptotic analysis, we developed the homogenized transmission conditions to be imposed on an interface plane representing the periodic perforation which, in reality, is featured by possibly complicated shapes of the obstacles forming the perforation. The further step in our research will be focused on solving an optimal perforation design problem to maximize the transmission loss.

8. Acknowledgments

This work is supported by projects GAČR 101/07/1471 and MSM 4977751303 of the Czech Republic.

9. References

- [1] E. Bangtsson, D. Noreland, M. Berggren, Shape optimization of an acoustic horn, *Comput. Methods Appl. Mech. Engrg.* vol. 192 pp. 1533-1571, 2003.
- [2] Cimrman, R. and others, SfePy home page, <http://sfepy.kme.zcu.cz>, 2008.
- [3] Haslinger, J., Neittaanmäki, P.: *Finite Element Approximation for Optimal Shape, Material and Topology Design*, 2nd ed. J. Wiley & Sons, Chichester, U.K., 1996.
- [4] Haug, E.J, Choi, K.K., Komkov, V. (1986) *Design Sensitivity Analysis of Structural Systems*, vol. 177, *Math. in Sci. and Engrg.*, Academic Press.
- [5] E. Rohan, V. Lukeš, Sensitivity analysis for the optimal perforation problem in acoustic trasmission. *Appl. Comp. Mech.*, Univ. West Bohemia, Pilsen, (accepted 2009)
- [6] E. Rohan and B. Miara. Homogenization and shape sensitivity of microstructures for design of piezoelectric bio-materials. *Mechanics of Advanced Materials and Structures* 13 (2006) 473-485.
- [7] E. Rohan, V. Lukeš, Homogenization of the acoustic transmission through perforated layer, *Jour. Appl. Math. Phys.*, (accepted 2008).

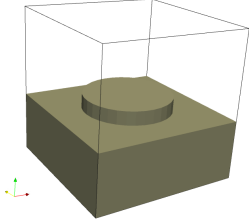
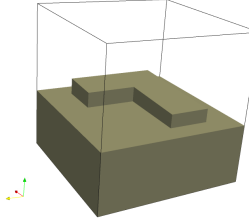
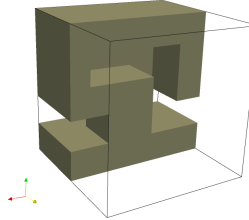
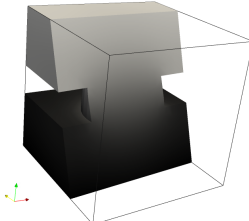
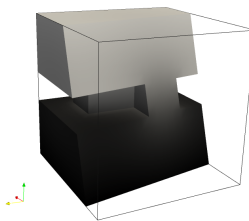
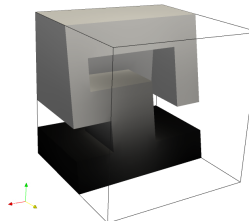
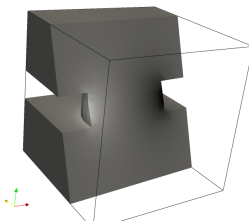
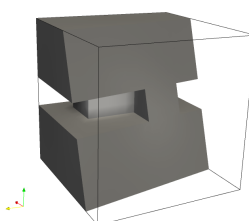
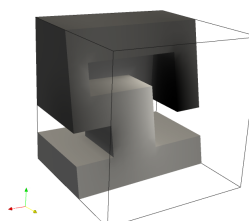
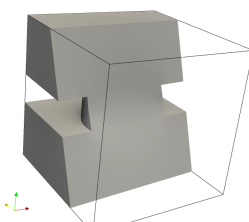
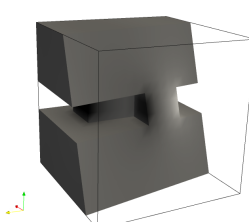
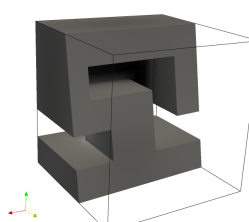
	Mic. 3D/#1	Mic. 3D/#2	Mic. 3D/#3
Geometry			
ξ^\pm			
π^1			
π^2			
A [(m/s) ²]	$\begin{bmatrix} 98415.75 & 0.0 \\ 0.0 & 98415.75 \end{bmatrix}$	$\begin{bmatrix} 98654.50 & 207.83 \\ 207.83 & 98155.32 \end{bmatrix}$	$\begin{bmatrix} 75295.34 & 0.0 \\ 0.0 & 81814.05 \end{bmatrix}$
B [m]	$[0.0 \ 0.0]$	$[0.0 \ 0.0]$	$[0.142330 \ 0.142330]$
F [s ²]	1.754429×10^{-5}	1.647584×10^{-5}	2.838839×10^{-5}

Figure 3: Distribution of the characteristic functions ξ^\pm , π^1 and π^2 in the microscopic domain Y^* and the homogenized acoustic coefficients for three shapes of 3D perforations.

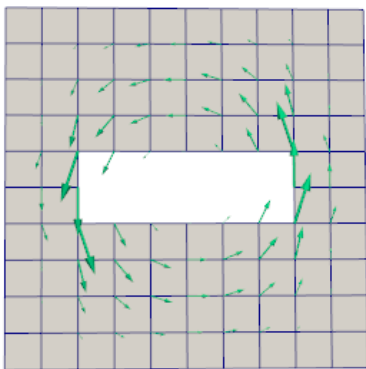
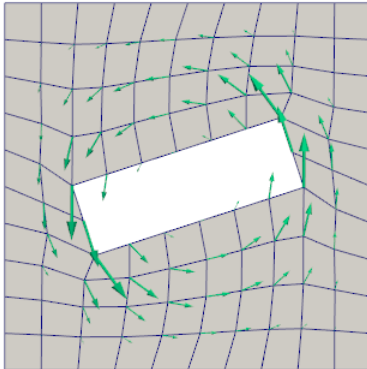
	No rotation	Rotated inclusion - $\varphi = \pi/10$
Design velocity field \mathcal{V}		
A [(m/s) ²]	99553.7109	96517.4395
δA	-335.5750	-18055.5925
B [m]	0.0	0.0928
δB	0.3338	0.2225
F [s ²]	1.3094×10^{-5}	1.2511×10^{-5}
δF	$-6.4800 \cdot 10^{-8}$	$-3.3897 \cdot 10^{-6}$

Figure 4: The shape sensitivity of the homogenized transmission coefficients A , B and F with respect to rotation of the embedded solid obstacle.